Available online www.jocpr.com

Journal of Chemical and Pharmaceutical Research, 2016, 8(5):644-650

Research Article

ISSN : 0975-7384
CODEN(USA) : JCPRC5

Studies on tautomeric stability, equilibrium and resonance of Derivatives Uracil: A DFT Study

M. Faal[a], A. Shameli[b*], E. Balali[a] and M. Monfared[a]

[a]*Department of Chemistry, Pharmaceutical Sciences Branch, Islamic Azad University, Tehran, Iran*
[b]*Department of Chemistry, Branch of Omidiyeh, Islamic Azad University, Omidiyeh, Iran*

ABSTRACT

We have studied the Uracil system with a set of 4,12b-Dihydro-3-thioxo-1H,7H-chromeno[4′,3′:4,5]pyrano[2,3-d]pyrimidine-1(2H)-one of different electronic features using several methods. Our aim is to find out a calculation method for the analysis of these molecules in biological systems. The combined IR and NBO study permitted us to justify the observed tautomeric preferences. The absolute predominance of the 2H-tautomer forms is greatly changed when the substituent group possesses anionic character; therefore the pH of the medium is relevant. When the calculations were carried out in solution, noteworthy changes in the behavior of charged substituents were observed. These facts may be relevant when studying the interactions of these molecules with biological receptors.

Keywords: Density Functional Theory, Uracil, tautomer, equilibrium, resonance

---

INTRODUCTION

Uracil is a common and naturally occurring pyrimidine derivative and one of the four nucleobases in the nucleic acid of RNA. In RNA, uracil binds to adenine via two hydrogen bonds. In DNA, the uracil nucleobase is replaced by thymine[1-3]. Uracil can be considered as a demethylated form of thymine. Uracil undergoes amide-imidic acid tautomeric shifts because any nuclear instability the molecule may have from the lack of formal aromaticity is compensated by the cyclic-amidic stability. The amide tautomer is referred to as the lactama structure, while the imidic acid tautomer is referred to as the lactim structure. These tautomeric forms are predominant at pH 7. The lactam structure is the most common form of uracil. Uracil is a weak acid. In RNA, uracil binds with a ribose sugar to form the ribonucleoside uridine. When a phosphate attaches to uridine, uridine 50- monophosphate is produced. There are many laboratory syntheses of uracil available. The first reaction is the simplest of the syntheses, by adding water to cytosine to produce uracil and ammonia [4]. The most common way to synthesize uracil is by the condensation of maleic acid with urea in fuming sulfuric acid [5]. Uracils are considered as privileged structures in drug discovery with a wide array of biological activities, synthetic accessibility and ability to confer drug like properties to the compound libraries appended on them at N^1, N^3, C^5 and C^6 positions (fig 1) [6]. Antiviral and anti-tumour are the two most widely reported activities of uracil analogues [7]; however they also possess herbicidal, insecticidal and bactericidal activities [8]. In the past two decades, a variety of synthetic methods have been employed for the preparation of functionalized uracils.

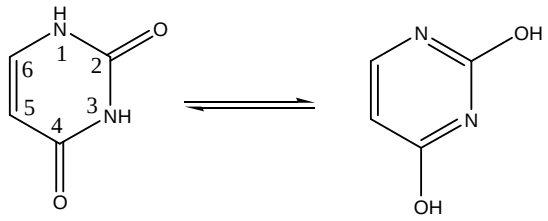

Fig 1: structure of tautomer uracil

The purpose of this study is to investigate molecular structure, vibrational frequencies (in gas phase), ^{1}H and ^{13}C NMR chemical shift values, NBO, NQR (in gas phase) and electronic absorption spectrum (in gas phase) for all five tautomeric forms, both theoretically. In addition to, the frontier molecular orbitals (FMOs or HOMOs and LUMOs) for all tautomers in the gas phase were studied at B3LYP/6-311++G(d,p) level.

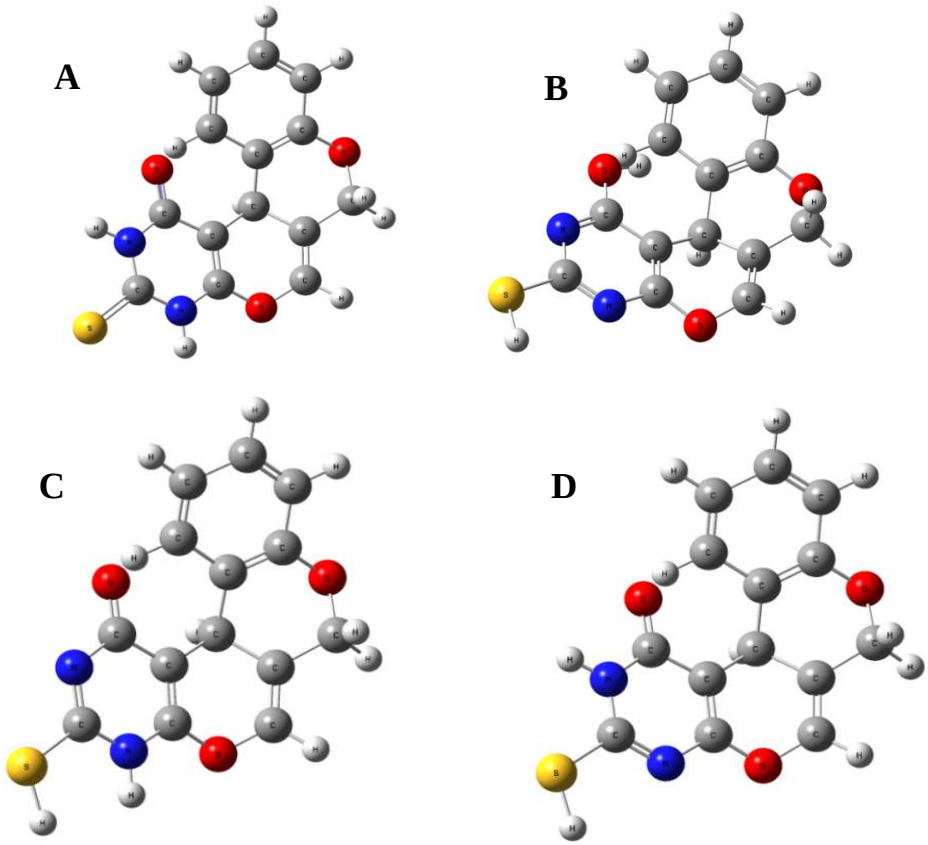

Fig. 2. The optimized molecular structures for all tautomers of 4,12b-Dihydro-3-thioxo-1H,7H-chromeno[4′,3′:4,5]pyrano[2,3-d]pyrimidine-1(2H)-one

Computational details and discussion:

We have performed density functional theory (DFT) calculations to optimize the structural models of tautomers of 4,12b-Dihydro-3-thioxo-1H,7H-chromeno[4′,3′:4,5]pyrano[2,3-d]pyrimidine-1(2H)-one systems has been studied in the gas. This reduces the computational cost in comparison to treating each molecule separately. All the structures were optimized at 6-311++G** level of theory. The B3LYP exchange‑correlation functional and the 6-31G/ standard basis set have been used to run all computations as implemented in the Gaussian 98 package [13]. It has been found that the NMR parameters calculated by B3LYP levels are in good agreement (fig2).

This work is to investigate the tautomers of 4,12b-Dihydro-3-thioxo-1H,7H-chromeno[4′,3′:4,5] pyrano[2,3-d]pyrimidine-1(2H)-one on the optimized structures and properties of thiouracil. To this aim, molecular and atomic properties (Tables 1 and 2) have been computationally evaluated for the investigated systems (Fig 2).

Table 1: Molecular properties model a-d

modelC		Model B		Model C		Model D	
Bond length (A^0)/ N1-C2	1.37	N1-C2	1.33	N1-C2	1.33	N1-C2	1.35
N1-C6	1.42	N1-C6	1.33	N1-C6	1.33	N1-C6	1.31
N1-H27	1.01	C2-N3	1.34	C2-N3	1.34	C2-N3	1.41
C2-N3	1.38	C2-S26	1.77	C2-S27	1.77	C2-S27	1.67
C2-S28	1.66	N3-C4	1.32	N3-C4	1.32	N3-C4	1.34
N3-C4	1.37	C4-C5	1.40	C4-C5	1.40	N3-H29	1.01
N3-H30	1.01	C4-O7	1.37	C4-O7	1.37	C4-C5	1.37
C4-C5	1.36	C5-C6	1.41	C5-C6	1.41	C4-O7	1.36
C4-O7	1.35	C5-C10	1.53	C5-C10	1.53	C5-C6	1.44
C5-C6	1.45	C6-O27	1.34	C6-O28	1.34	C5-C10	1.53
C5-C10	1.52	O7-C8	1.39	O7-C8	1.39	C6-O28	1.34
C6-O29	1.22	C8-C9	1.33	C8-C9	1.33	O7-C8	1.40
O7-C8	1.39	C8-H19	1.08	C8-H19	1.08	C8-C9	1.33
C8-C9	1.33	C9-C10	1.52	C9-C10	1.52	C8-H19	1.08
C8-H19	1.08	C9-C13	1.49	C9C13	1.49	C9-C10	1.52
C9-C10	1.51	C10-C11	1.52	C10-C11	1.52	C9-C13	1.50
C9-C13	1.49	C11-C12	1.41	C10-H20	1.10	C10-C11	1.52
C10-C11	1.54	C11-C18	1.40	C11-C12	1.41	C10-H20	1.10
C10-H20	1.10	C12-O14	1.37	C11-C18	1.40	C11-C12	1.41
C11-C12	1.41	C12-C15	1.40	C12-O14	1.37	C11-C18	1.40
C11-C18	1.40	C13-O14	1.43	C12-C15	1.40	C12-O14	1.37
C12-O14	1.38	C13-H21	1.09	C13-O14	1.43	C12-C15	1.40
C12-C15	1.40	C13-H22	1.10	C13-H21	1.09	C13-O14	1.43
C13-O14	1.43	C15-C16	1.39	C13-H22	1.10	C13-H21	1.09
C13-H21	1.10	C15-H23	1.08	C15-C16	1.39	C13-H22	1.10
C13-H22	1.09	C16-C17	1.40	C15-H23	1.08	C15-C16	1.39
C15-C16	1.39	C16-H24	1.08	C16-C17	1.40	C15-H23	1.08
C15-H23	1.08	C17-C18	1.39	C16-H24	1.08	C16-C17	1.40
C16-C17	1.39	C17-H25	1.08	C17-C18	1.39	C16-H24	1.08
C16-H24	1.09	C18-H30	2.22	C17-H26	1.08	C17-C18	1.39
C17-C18	1.39	S26-H28	1.35	C18-H25	2.22	C17-H26	1.08
C17-H26	1.08	O27-H29	2.68	S27-H29	1.35	C18-H25	2.22
C18-H25	1.08	C2N1C6	117.27	O28-H30	2.68	C18-H30	1.09
Bond Angel/C2N1C6	127.95	N1C2N3	126.73	C2N1C6	117.27	C2N1C6	121.64
C2N1H27	116.49	N1C2S26	114.79	N1C2N3	126.73	N1C2N3	115.73
C6N1H27	115.52	N3C2S26	118.46	N1C2S27	114.80	N1C2S27	125.62
N1C2N3	112.84	C2N3C4	114.27	N3C2S27	118.45	N3C2S27	118.62
N1C2S28	124.55	N3C4C5	125.43	C2N3C4	114.26	C2N3C4	121.78
N3C2S28	122.61	C3C4O7	115.10	N3C4C5	125.44	C2N3H29	117.74
C2N3C4	123.72	C5C4O7	119.43	N3C4O7	115.10	C4N3H29	120.40
C2N3H30	117.18	C4C5C6	113.31	C5C4O7	119.43	N3C4C5	122.20
C4N3H30	119.09	C4C5C10	113.84	C4C5C6	113.31	N3C4O7	115.23
N3C4C5	123.19	C6C5C10	132.84	C4C5C10	113.84	C5C4O7	122.53
N3C4O7	111.24	N1C6C5	121.93	C6C5C10	132.84	C4C5C6	112.91
C5C4O7	125.54	N1C6O27	113.89	N1C6C5	121.93	C4C5C10	112.96
C4C5C6	116.92	C5C6O27	124.17	N1C6O28	113.90	C6C5C10	134.11
C4C5C10	120.93	C4O7C8	115.16	C5C6O28	124.18	N1C6C5	123.87
C6C5C10	121.57	O7C8C9	120.72	C4O7C8	115.15	N1C6O28	114.50
N1C6C5	114.91	O7C8H19	111.96	O7C8C9	120.72	C5C6O28	121.61
N1C6O29	119.28	C9C8H19	127.21	O7C8H19	111.96	C4O7C8	114.28
C5C6O29	125.80	C8C9C10	115.98	C9C8H19	127.21	O7C8C9	120.15
C4O7C8	116.40	C8C9C13	124.82	C8C9C10	115.98	O7C8H19	111.54
O7C8C9	123.68	C10C9C13	118.68	C8C9C13	124.82	C9C8H19	128.16
O7C8H19	110.13	C5C10C9	105.49	C10C9C1	118.68	C8C9C10	116.70
C9C8H19	126.19	C5C10C11	121.93	C5C10C9	105.49	C8C9C13	124.16
C8C9C10	123.21	C5C10H20	104.68	C5C10C11	121.93	C10C9C13	118.68
C8C9C13	122.42	C9C10C11	112.76	C5C10H20	104.68	C5C10C9	105.75
C10C9C13	113.65	C9C10H20	105.71	C9C10C11	112.77	C5C10C11	121.57
C5C10C9	109.13	C11C10H20	104.92	C9C10H20	105.71	C5C10H20	105.16

C5C10C11	117.47	C10C11C12	119.92	C11C10H20	104.92	C9C10C11	112.71
C5C10H20	107.36	C10C11C18	121.60	C10C11C12	119.91	C9C10H20	105.66
C9C10C11	106.46	C12C11C18	117.66	C10C11C18	121.60	C11C10H20	104.72
C9C10H20	108.95	C11C12O14	122.97	C12C11C18	117.66	C10C11C12	119.90
C11C10H20	107.24	C11C12C15	120.74	C11C12O14	122.97	C10C11C18	121.57
C10C11C12	119.12	O14C12C15	116.18	C11C12C15	120.74	C12C11C18	117.66
C10C11C18	123.00	C9C13O14	112.83	O14C12C15	116.18	C11C12O14	122.82
C12C11C18	117.88	C9C13H21	112.46	C9C13O14	112.83	C11C12C15	120.83
C11C12O14	124.37	C9C13H22	109.74	C9C13H21	112.46	O14C12C15	116.22
C11C12C15	120.75	O14C13H21	106.08	C9C13H22	109.74	C9C13O14	112.84
O14C12C15	114.88	O14C13H22	107.45	O14C13H21	106.08	C9C13H21	112.47
C9C13O14	110.38	H21C13H22	108.02	O14C13H22	107.45	C9C13H22	109.30
C9C13H21	110.59	C12O14C13	116.29	H21C13H22	108.02	O14C13H21	106.18
C9C13H22	112.83	C12C15C16	120.27	C12O14C13	116.29	O14C13H22	107.79
O14C13H21	108.51	C12C15H23	118.27	C12C15C16	120.27	H21C13H22	108.04
O14C13H22	105.81	C16C15H23	121.45	C12C15H23	118.27	C12O14C13	116.22
H21C13H22	108.53	C15C16C17	120.01	C16C15H23	121.45	C12C15C16	120.19
C12O14C13	118.17	C15C16H24	119.70	C15C16C17	120.01	C12C15H23	118.31
C12C15C16	120.18	C17C16H24	120.29	C15C16H24	119.69	C16C15H23	121.49
C12C15H23	118.30	C16C17C18	119.46	C17C16H24	120.29	C15C16C17	120.01
C16C15H23	121.52	C16C17H25	120.60	C16C17C18	119.46	C15C16H24	119.70
C15C16C17	119.93	C18C17H25	119.94	C16C17H26	120.60	C17C16H24	120.28
C15C16H24	119.64	C11C18,C17	121.75	C18C17H26	119.94	C16C17C18	119.52
C17C16H24	120.42	C17C18H30	117.32	C17C18H25	117.34	C16C17H26	120.59
E(Kev)	-34.644		-34.643		-34.643		-34.642
Dipol Moment (Debay)	4.3355		3.1047		7.2485		4.5695

Table2: parameters NBO analysis

Atom Number	Charge	Core	Valence	Rydberg	Total
N1	-0.60007	1.99923	5.58444	0.01640	7.60007
C2	0.34412	1.99919	3.61971	0.03697	5.65588
N3	-0.55096	1.99917	5.53014	0.02165	7.55096
C4	0.56567	1.99870	3.40384	0.03179	5.43433
C5	-0.21466	1.99883	4.19790	0.01794	6.21466
C6	0.64341	1.99918	3.31400	0.04341	5.35659
O7	-0.49682	1.99969	6.47678	0.02035	8.49682
C8	0.17148	1.99864	3.80472	0.02515	5.82852
C9	-0.10392	1.99898	4.08819	0.01674	6.10392
C 10	-0.25081	1.99905	4.22910	0.02266	6.25081
C 11	-0.09181	1.99892	4.07603	0.01687	6.09181
C 12	0.31706	1.99866	3.66095	0.02332	5.68294
C 13	-0.02419	1.99908	4.00284	0.02228	6.02419
O 14	-0.55211	1.99973	6.53329	0.01909	8.55211
C 15	-0.23611	1.99906	4.21839	0.01866	6.23611
C 16	-0.18606	1.99916	4.16891	0.01799	6.18606
C 17	-0.22235	1.99916	4.20426	0.01893	6.22235
C 18	-0.17724	1.99907	4.16080	0.01737	6.17724
H 19	0.19766	0.00000	0.80137	0.00097	0.80234
H 20	0.23504	0.00000	0.76174	0.00321	0.76496
H 21	0.17993	0.00000	0.81829	0.00177	0.82007
H 22	0.19446	0.00000	0.80438	0.00116	0.80554
H 23	0.21566	0.00000	0.78324	0.00110	0.78434
H 24	0.20309	0.00000	0.79624	0.00066	0.79691
H 25	0.21834	0.00000	0.78037	0.00129	0.78166
H 26	0.20325	0.00000	0.79602	0.00073	0.79675
H 27	0.41461	0.00000	0.58159	0.00380	0.58539
S 28	0.06285	9.99917	5.90497	0.03301	15.93715
O 29	-0.62365	1.99976	6.61130	0.01259	8.62365
H30	0.16413	0.00000	0.83321	0.00265	0.83587
* Total *	0.00000	47.98244	99.54701	0.47054	148.00000

The structure of A molecule is defined by the point group C_1 angles which determine the orientation of the branches and terminal groups. Although the comparison between the structures in the gas phase. Calculated bond lengths (in

Å) 1.01-1.77 and bond angles (in degrees) 105-127. In this work, the keto-enol tautomerizations of the four structures are discussed by comparing their relative equilibrium constants.

NBO theory allows investigating the conjugated interactions in molecular systems, and is an effective method for studying intermolecular interactions. The second-order Fock matrix was carried out to evaluate the donor-acceptor interactions in NBO analysis (table 2).

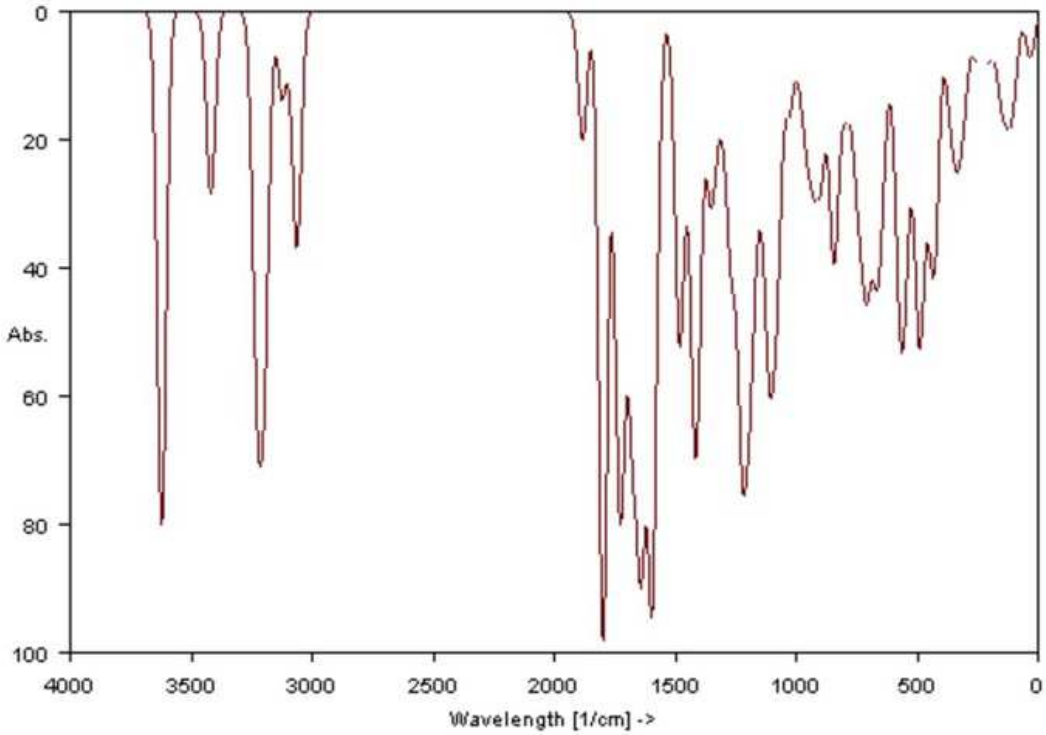

Fig3: spectrum IR Molecule A

Table 3: IR spectra and relative intensity spectra of A

frequency (cm^{-1})	intensity	frequency (cm^{-1})	intensity
3626	31.91	1411	36.51
3620	50.9	1265	26.72
3419	29.13	1230	33.01
3232	45.22	1219	25.23
3206	38.22	1192	34.34
3190	22.82	1149	19.45
3066	23.65	1115	40.72
1882	20.34	1094	21.6
1798	100	1075	28.07
1738	40.76	925	18.95
1719	50.63	895	21.67
1677	59.02	848	25.03
1640	78.85	712	33.5
1596	89.24	662	29.35
1478	43.47	492	38.58
1429	30.42	424	24.46

Calculation of dendrimer molecules with the DFT theoretical spectra. This increases the accuracy of the interpretation of bands in the entire frequency range in which the spectra were recorded. Within the present study the use of IR spectroscopy in conjunction with computational methods in quantum chemistry is interesting from the point of view of obtaining unique information that helps to better understand the structure of dendrimers. The interpretation of IR spectra of zero generation allows determining the local changes in the structure. in the IR

spectrum of A are asymmetric and symmetric NH stretching vibrations of amid group. The experimental frequencies of these bands are lower than theoretical values due to intramolecular N\\H···S hydrogen bond. This hydrogen bond is also responsible for higher experimental infrared(table 3).

The energies of highest occupied molecular orbital (HOMO) and the lowest unoccupied molecular orbital (LUMO) were calculated using 6-311++G(d,p) method and the pictorial illustration of the frontier molecular orbitals of A are shown in Fig. 4.

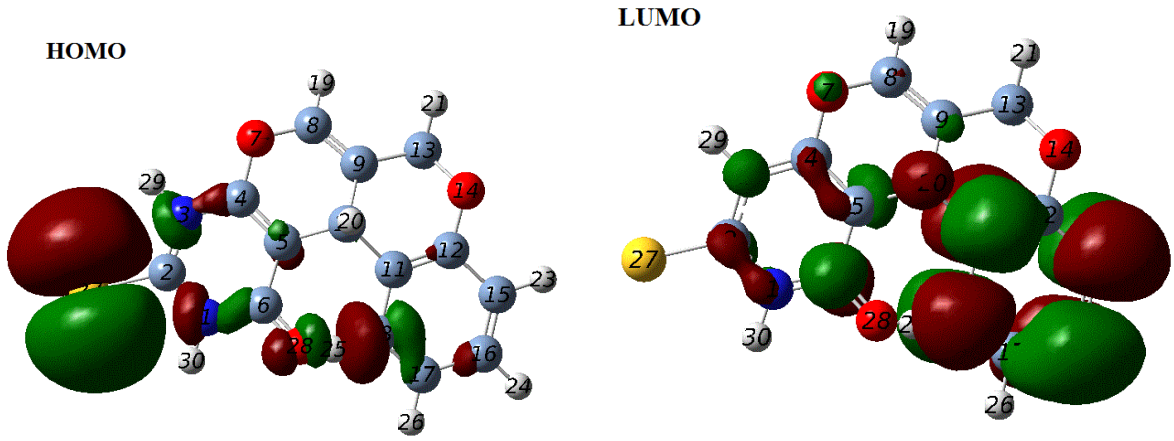

Fig 4: Molecular orbital surfaces of A

CONCLUSION

Initial quantum mechanic studies and density function theory (DFT) in the level of B3LYP/6-311++G** on Keto-Enol Tautomerism process 4,12b-Dihydro-3-thioxo-1H,7H-chromeno [4′,3′:4,5]pyrano[2,3-d]pyrimidine-1(2H)-one structure, that results shows that activation energy for this reaction equal 34.6 (keV.mol^{-1}). The process is a type of easy and fast balance that is more stabler of enol state. The results of NBO analysis of showed that the bond are in resonance condition with pair electrons nonbonding atom O, S and therefore providing enol state that is a kind of isomeric reaction and the intermediate in these reactions usually is the structure between ketone and enol state. Bond angels and density of electrons aren't the same in structures enol state, transition state and ketone state. Also tautomerism is a kind of endothermic isomeric reaction. sets.

Acknowledgment
The authors are grateful to the Department of Chemistry, Pharmaceutical Sciences Branch, Islamic Azad University, Tehran, Iran for the financial support.

REFERENCES

[1] Z. Martins, O. Botta, M.L. Fogel, M.A. Sephton, D.P. Glavin, J.S. Watson, J.P. Dworkin, A.W. Schwartz, P. Ehrenfreund, *Earth Planet. Sci. Lett*. **2008**, 270, 130-136.
[2] R.L. Myers, The 100 Most Important Chemicals Compounds, Greenwood Publishing Group Inc, **2007**, 92-93.
[3] A. Clark, N. Pearson, R.H. Brown, D.P. Cruikshank, J. Barnes, R. Jaumann, L. Soderblom, C. Griffith, P. Rannou, S. Rodriguez, S. Le Mouelic, J. Lunine, C. Sotin, K.H. Baines, B.J. Buratti, P.D. Nicholson, R.M. Nelson, K. Stephan, The surface composition of titan, Am. Astronomical Soc. (Smithsonian/NASA Astrophysics Data Syst.) **2012,**44.
[4] H.R. Garrett, C.M. Grisham, Principals of Biochemistry with a Human Focus, Cole Thomson Learning, **1997**.
[5] D.J. Brown, Heterocyclic Compounds, vol. 52, Interscience, New York, **1994**.
[6] G.R. Newkome, W.W. Pandler, Contemporary Heterocyclic Chemistry, Wiley, New York, **1982**.
[7] (a) W.B. Parker, *Chem. Rev*. **2009**,109, 2880e2893; (b) T. Pathak, *Chem. Rev*. **2002**,102, 1623-1668 c) S.Shojaei, A.Shameli, E. Balali, R. Khadivi. *Orient. J. Chem*., **2016**, 32(1), 291- 294.
[8] (a) R. Soladino, C. Crestini, A.T. Palamara, M.C. Danti, F. Manetti, F. Corelli, E. Garaci, M. Botta, J. Med. Chem. **2001**,44, 4554-4562; (b) C. Zhi, Z. Long, A. Manikowski, N.C. Bron, P.M. Tarantino, K. Holm, E.J. Dix,

G.E. Wright, K.A. Foster, M.M. Butler, W.A. LaMarr, D.J. Skow, I. Motorina, S. Lamothe, R. Storer, J. Med. Chem. **2005**,48, 7063-7074; (c) S. Fustero, J. Piera, J.F. Sanz-Cervera, S. Catalan, A.C. Ramirez, Org. Lett. **2004**,6 ,1417-1420; (d) K.S. Jain, T.S. Chitre, P.B. Minutosiyar, M.K. Kathiravan, V.S. Bendre, V.S. Veer, R.S. Shahane, C.J. Shishoo, *Curr. Sci*. **2006**,90, 793-803.
[9] N.F. Smith, W.D. Figg, A. Sparreboom, *Drug Dev. Res*. **2004**,62, 233-253.
[10] L.M. Zhao, L.M. Zhang, J.J. Liu, L.J. Wan, Y.Q. Chen, S.Q. Zhang, Z.W. Yan, J.H. Jiang, *Eur. J. Med. Chem*. **2012,** 47, 255-260.
[11]a) A.A. Arutyunyan, S.S. Mamyan, H.M. Stepanyan, R.V. Paronikyan, *Pharm. Chem. J*. **2013**, 47, 303-306. b) E.Balali, A.Shameli, H.Naeimi, M. M. Ghanbari *Orient. J. Chem*., **2013**, 29(4), 1611-1614. C) J.Azizian, A. Shameli, S.Balalaie, M. M. Ghanbari, S.Zomorodbakhsh, M.Entezari, S.Bagheri, G. Fakhrpour Orient. J. Chem., **2012**, 28(1), 327-332 d) S. Balalaie, J.Azizian, A., Shameli H.R. Bijanzadeh. Synthetic Commun. **2013**, 43, 1787–1795 e) A.Shameli Akandi, E. Balali, T.Mosavat, M. M.Ghanbari, A. Eazabadi. *Orient. J. Chem*., **2014**, 30(2), 587-591. F) J Azizian, A Shameli, S Balalaie, S. Zomorodbakhsh *Orient. J. Chem*., **2012**, 28(1), 221-227.g)
[12] M.J. Frisch, G.W. Trucks, H.B. Schlegel, G.E. Scuseria, M.A. Robb, J.R. Cheeseman, V.G. Zakrzewski, J.A. Montgomery, R.E. Stratmann, J.C. Burant, S.Dapprich, J.M. Millam, A.D. Daniels, K.N. Kudin, M.C. Strain, O. Farkas, J. Tomasi, V. Barone, M. Cossi, R. Cammi, B. Mennucci, C. Pomelli, C. Adamo, S.Clifford, J. Ochterski, G.A. Petersson, P.Y. Ayala, Q. Cui, K. Morokuma, D.K. Malick, A.D. Rabuck, K. Raghavachari, J.B. Foresman, J. Cioslowski, J.V. Ortiz, A.G. Baboul, B.B. Stefanov, G. Liu, A. Liashenko, P. Piskorz, I. Komaromi, R. Gomperts, R.L. Martin, D.J. Fox, T. Keith, M.A. Al-Laham, C.Y. Peng, A. Nanayakkara, C. Gonzalez, M. Challacombe, P.M.W. Gill, B. Johnson, W. Chen, M.W. Wong, J.L. Andres, C. Gonzalez, M. Head-Gordon, E.S. Replogle, J.A. Pople, Gaussian 98, Revision A.7, Gaussian Inc, Pittsburgh, PA **1998**.